Available online at www.sciencedirect.com
SCIENCE DIRECT®
Journal of Sound and Vibration 272 (2004) 21–38
JOURNAL OF SOUND AND VIBRATION
www.elsevier.com/locate/jsvi

Quenching of vortex-induced vibrations of towering structure and generation of electricity using Hula-Hoops

Y. Yoshitake[a,*], A. Sueoka[b], M. Yamasaki[c], Y. Sugimura[d], T. Ohishi[e]

[a] *Department of Structural Engineering, Nagasaki University, 1-14 Bunkyoumachi, Nagasaki 852-8521, Japan*
[b] *Kyushu University, 6-1-1 Hakozaki Higashi-ku, Fukuoka 812-8581, Japan*
[c] *Namura Ship-building Co. Ltd, 5-1 Shioya Kurokawachou, Imari, Saga 848-0121, Japan*
[d] *Daifuku Co. Ltd, 3-2-11 Mitejima Nishiyodogawa-ku, Osaka 555-0012, Japan*
[e] *Graduate Student, Nagasaki University, Japan*

Received 10 June 2002; accepted 17 March 2003

Abstract

This paper deals with the quenching problem of vortex-induced vibrations by using devices composed of Hula-Hoops and generators. These devices are also able to generate electricity. The experiment was made concerning the quenching problem of the vortex-induced vibrations of towering structures with the devices. Moreover, a numerical analysis was also carried out using the Runge–Kutta–Gill method. An optimum approach for quenching the vortex-induced vibrations of low and high flexural rigidity directions are discussed. As a result, the following was made clear: (1) The vortex-induced vibrations of both flexural rigidity directions were well quenched for a wide range of wind velocities and the different wind directions by using four devices simultaneously. (2) The optimally quenched vibration was a chaos of intermittency. (3) A condition of maximum power generation was not equal to that of the optimum vibration quenching of the main system. (4) The experimental and the analytical results were in good qualitative agreement with each other.

1. Introduction

The vortex-induced vibration of structures is an important engineering problem and has been researched for many years. Many mathematical models of vortex-induced vibration of structures have been proposed comparing experimental results. Birkhoff [1] proposed the wake oscillator model first, and it was developed by Funakawa [2], Hartlen and Currie [3], Skop and Griffin [4],

*Corresponding author. Tel.: +81-95-847-1111; fax: +81-95-843-7464.
E-mail address: yoshitak@st.nagasaki-u.ac.jp (Y. Yoshitake).

0022-460X/03/$ - see front matter
doi:10.1016/S0022-460X(03)00304-3

Iwan and Blevins [5], Dowell [6] and so on. Hartlen and Currie, Skop and Griffin, and Dowell used the lift coefficient in their models. In the model of Hartlen and Currie and that of Skop and Griffin, the consideration for the interaction between the structure and the lift force is not enough. Dowell's model is a little complex. Iwan and Blevins used the average transverse component of fluid velocity, and it is considered that the interaction between the structure and the lift force is suitable in the model. In recent years, many studies about the quenching of vortex-induced vibration were also performed. These are divided into two categories, namely, passive control by eliminating the vortex shedding and using a dynamic absorber, and active control by using an actuator. Concerning the first category, there is the research by Hanko [7], Walshe and Woolton [8], and Andersen et al. [9]. In the latter, there is the research by Nishioka et al. [10], Baz and Ro [11], Venkatraman and Narayanan [12], and Gattulli and Ghanem [13]. However, in the active control, external power is needed to move the actuator.

On the contrary, the authors have studied the vibration quenching and power generating device [14]. In the previous paper [14], the quenching problem of self-excited vibration generated in a machine or a structure, such as a frictional vibration and a vortex-induced vibration, was treated. The vibration quenching and power generating device which consists of a Hula-Hoop and a generator was designed, and fundamental research about quenching the one-degree-of-freedom self-excited system and generating electricity using the vibration energy was performed. As a result, it was clarified that it can quench vibration and simultaneously generate electricity by using this device, and that the oscillating state at the time of optimum quenching was chaos. Moreover, the design conditions of this device, when the optimum quenching of self-excited vibration was prior to generation, were clarified.

The vortex-induced vibration of the structure is treated in this paper. As the wind velocity and the frequency of vortex-induced vibration may change depending on the direction of the wind because of the anisotropic flexural rigidity, it is necessary to perform the measure. Moreover, the validity of the quenching device in a wide range of wind velocities also needs to be checked. Therefore, in this report, considering the model of a towering structure near an actual structure, the problem about quenching vortex-induced vibration and generating power more efficiently using two or more of these devices, is dealt with. Here, the vibration control is the first purpose and generating electricity is the second. Considering the model of a towering structure whose two flexural rigidities are different from each other as a two-degree-of-freedom system and adopting the vortex-induced model by Iwan and Blevins [5], the validity of this device to the wide wind velocity range and the change of wind direction is investigated.

2. Experimental result

In this section, the possibility of quenching a vortex-induced vibration of a towering structure and electricity generation using the devices consisting of Hula-Hoops and generators is shown by experimentation.

The experimental apparatus is shown in Fig. 1. The measurement section of a wind tunnel with a height $\times$ width $= 400\,\text{mm} \times 300\,\text{mm}$ is used. The main system is composed of an aluminum cylinder and a vertical steel beam fixed to the center axis of the cylinder, and the lower end of the beam is fixed to the bottom of the wind tunnel. The length, its outer diameters and the thickness of

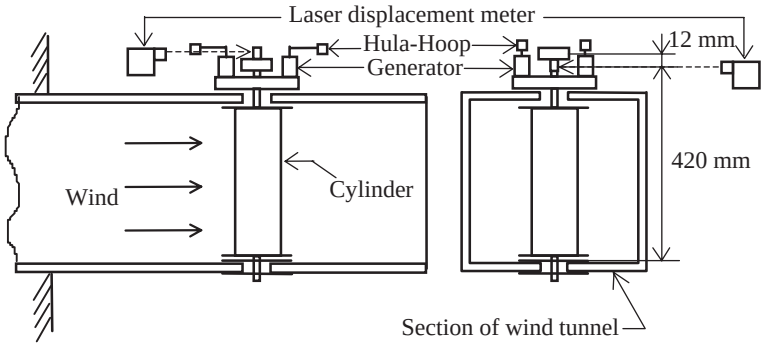

Fig. 1. Experimental apparatus.

the cylinder are 365, 83, and 0.2 mm, respectively. The length of the beam is 450 mm and its cross-section is rectangular with 3 mm × 4 mm dimensions. Therefore, the flexural rigidity of the beam is anisotropic. The mass M of the main system is 0.200 kg. The lower rigid direction of the two bending directions of the main system is defined as x and the higher rigid direction is defined as y. The measured natural frequency of the x direction is $f_x = 4.9$ Hz and that of the y direction is $f_y = 6.0$ Hz.

In order to quench the vortex-induced vibration efficiently, four passive vibration-quenching and electricity-generating devices are installed in the main system. Each device is composed of a Hula-Hoop and a generator. The reason for using these four devices is as follows: if only one device is attached in a towering structure which can vibrate not only in the perpendicular direction to the wind but also in the same direction of the wind, the structure may vibrate along the direction of the wind by the centrifugal force of a Hula-Hoop. Therefore, if one set composed of two Hula-Hoops is attached in a position parallel to the wind direction and rotate mutually in a reverse direction, the wind direction ingredients of the centrifugal forces generated by the rotation of two Hula-Hoops may be negated by each other, and the vibration of the wind direction does not arise. Moreover, when the wind blows from a different direction, if this device operates as one pair similarly, the ingredients in the wind direction of the centrifugal forces can be cancelled. For these reasons, two or more of these devices of the completely same structure are used. As an example, the four devices that are the minimum number needed in the towering structure with rectangular sections are adopted in the experiment.

In a previous report [14] concerning the problem of quenching self-excited vibration with only one device, the optimum values of the device are as follows:

$$\mu = m/M \fallingdotseq 0.06, \quad \lambda = (I/mA^2)^{1/2} = 0.2-0.3, \quad \delta = 1/A \fallingdotseq 0.5,$$
$$\gamma = c/(M\omega A^2) = 0.7 \times 10^{-3} - 0.9 \times 10^{-3},$$

where, as shown in Table 1, m is the mass of the Hula-Hoop, I is the inertia of moment about the center of gravity of the Hula-Hoop, l is the length from the center of gravity of a Hula-Hoop to the rotation center (henceforth, it is called stem length), A and ω are the amplitude and the angular velocity of vortex-induced vibration, c is the damping coefficient of the Hula-Hoop. In this report, five kinds of Hula-Hoops, types A–E are used in the experiment. Hula-Hoop C is designed referring to the above optimum values. Generators are direct-current motors rated

Table 1
Figure of the Hula-Hoops

Hula-Hoop	m (kg)	I (kg/m^2)	l (m)
A	3.00×10^{-4}	3.66×10^{-9}	7.71×10^{-3}
B	8.00×10^{-4}	2.31×10^{-8}	1.02×10^{-2}
C	2.00×10^{-3}	2.14×10^{-8}	7.50×10^{-3}
D	2.00×10^{-3}	9.34×10^{-8}	1.30×10^{-2}
E	3.40×10^{-3}	1.71×10^{-7}	1.67×10^{-2}

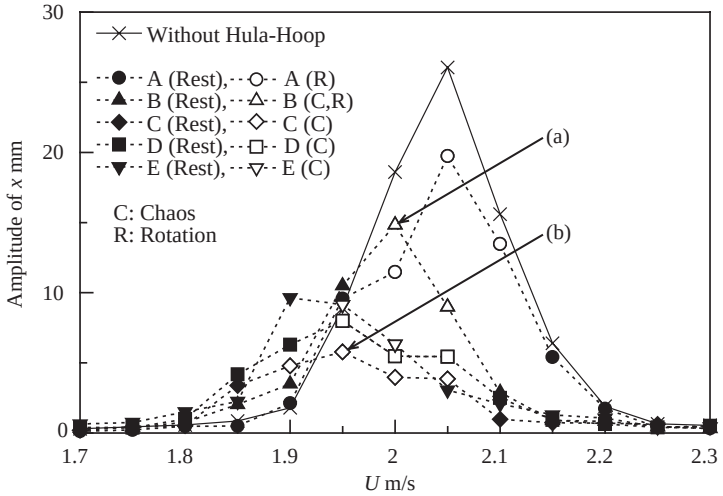

Fig. 2. Wind response curve (experiment: low rigidity direction).

7500 rpm and 0.078 W (TYPE 6CH-1201WL-00 by Namiki Motor Company). The coefficient of viscous damping corresponding to the load torque for power generation was measured from the deceleration of free rotation of the Hula-Hoop. The result is $c = 7.5 \times 10^{-7}$ N m/s. The displacements of the x, y directions of the main system are measured using two laser displacement meters and two small reflective plates as shown in Fig. 1. Resistance of $R_f = 1.0\,\Omega$ is connected to both terminals of each generator and the voltage $E_i(V)$ between terminals are measured ($i = 1, \ldots, 4$). The amount of power generation $P(W)$ is calculated as follows using the average value $\bar{E}_i$(V) ($i = 1, \ldots, 4$).

$$P = \sum_{i=1}^{4} \overline{E_i}^2 / R_f. \tag{1}$$

At first, the vortex-induced vibration generated in the low flexural rigidity direction of the structure was considered. The relation between the wind velocity and the amplitude of the main system is shown in Fig. 2. The relation between the wind velocity and the amount of power generated is shown in Fig. 3. In the aperiodic vibration, the averaged values from sufficiently long data (for 80 s) are adopted. Namely, the amplitude of displacement is calculated as one half of the difference of the averaged value of the local maximum and the averaged value of the local

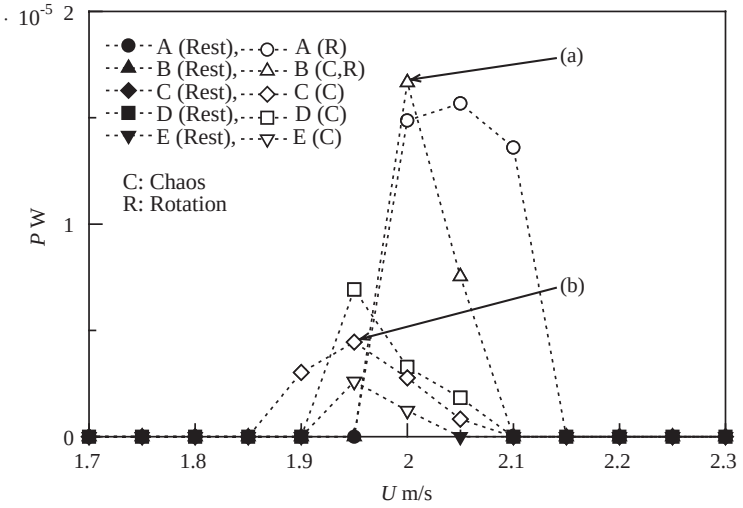

Fig. 3. Electric power (experiment: low rigidity direction).

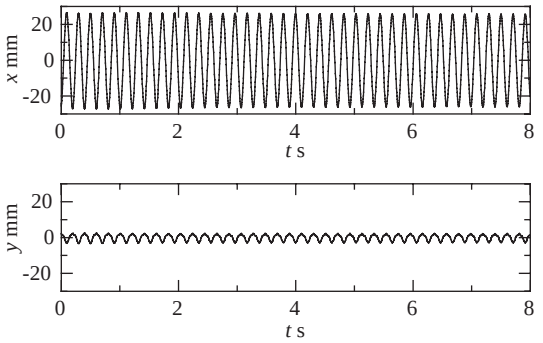

Fig. 4. Experimental waveform of a main system without Hula-Hoops.

minimum. In Figs. 2 and 3, the kinds of Hula-Hoops are expressed with A–E. The marks coated inside mean the cases where Hula-Hoops continue to stand still, and this is shown as "Rest" in the figures. The marks not-coated inside mean the cases where Hula-Hoops do not continue to stand still. About the latter cases, "C" and "R" in the figures mean the chaos and the steady state rotation of a Hula-Hoop, respectively. When the Hula-Hoops are not attached, the lock-in region is the region of wind velocity 1.95–2.15 m/s and the maximum amplitude of displacement is 26.0 mm in the wind velocity $U = 2.05$ m/s. Its waveform is shown in Fig. 4. It appears from Fig. 4 that a vibration of a high rigidity direction arises very slightly when a Hula-Hoop is not equipped.

In Fig. 2, although the amplitude of a main system changes depending on the wind velocity, the main system is quenched by the vibration and rotation of the Hula-Hoops in some ranges of wind velocity where the amplitude of the main system becomes larger than some value. Hula-Hoop C is the best one among the five Hula-Hoops in Fig. 2, and the amplitude is quenched less than 25% of the maximum amplitude in case of having no quenching device over the wind velocities.

In Hula-Hoop C which is the optimum for quenching, the amount of power generation is slight as shown in Fig. 3. On the other hand, the amount of power generation is large in Hula-Hoops A and B which have a smaller quenching effect. The amount of power generated is large in $U = 2.00-2.10$ m/s of Hula-Hoop A and $U = 2.00$ m/s of Hula-Hoop B because Hula-Hoops rotate steady in these wind velocities.

The typical waveforms in Figs. 2 and 3 are shown in Fig. 5. These are the waveforms at the maximum amplitude of displacement in the wind response curves. From the top in order, these are waveforms of the displacement of x direction of the main system, that of y direction, and the waveforms of generating voltage of the four Hula-Hoops. One set of two pieces of Hula-Hoops indicated by the subscripts 1 and 2, and the other set indicated by the subscripts 3 and 4 are attached parallel to the wind direction. Also, if a Hula-Hoop rotates regularly and a descent of the brush contact voltage of a generator is approximated with zero, there is the following

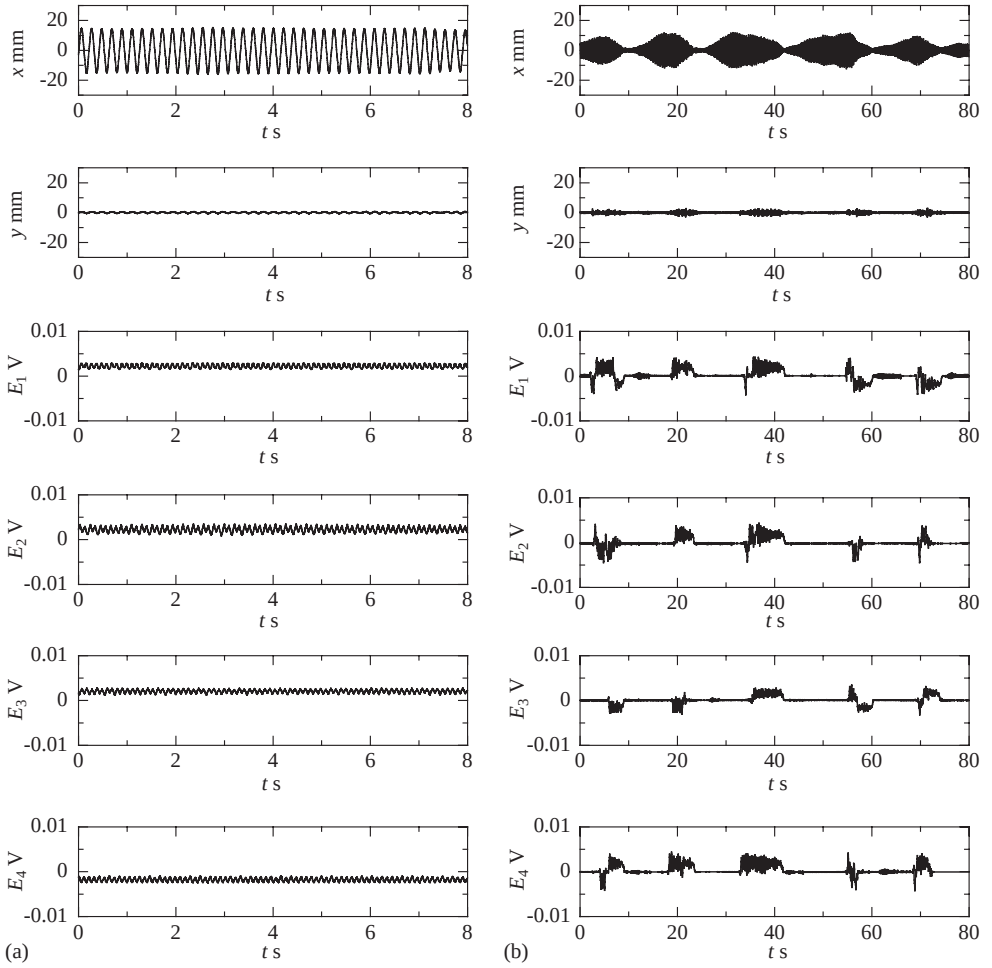

Fig. 5. Experimental waveforms with Hula-Hoops: (a) periodic solution (Hula-Hoop B, $U = 2.00$ m/s); (b) chaos (Hula-Hoop C, $U = 1.95$ m/s).

proportional relations between the rotational angular velocity $\dot{\theta}_i$ of a generator and voltage between terminals E_i $(i = 1, \ldots, 4)$ [15].

$$E_i = K_{E_i} R_f \dot{\theta}_i / (R_{a_i} + R_f), \tag{2}$$

where K_{E_i} and R_{a_i} are the reverse electromotive power constant of a generator, and coil resistance, respectively. If this proportional relation between the measured voltage E_i and the rotational angular velocity $\dot{\theta}_i$ of a generator is considered, it is thought that each measured voltage E_i in Fig. 5 is approximately proportional to the angular velocity of a Hula-Hoop $\dot{\theta}_i$. Although every Hula-Hoop rotates in one direction in Fig. 5(a) and generates electricity steadily, it remains in about 40% reduction of amplitude as a quenching effect. Waveforms of Fig. 5(b) show an unsteady motion where Hula-Hoops repeat aperiodically stand still, vibration, and rotation. The correlation dimension calculated using the waveform of the main system is shown in Fig. 6. The inclination converges when the embedding dimension is more than three in the figure, and the correlation dimension occurs with $D_c \fallingdotseq 1.87$. As the correlation dimension D_c is a non-integer, it becomes evident that Fig. 5(b) is chaos. The lock-in is degenerated by the chaotic motion of the Hula-Hoops and the averaged amplitude of a main system becomes small. Although one set of two pieces of the Hula-Hoops may rotate in the opposite direction, or in the same direction as shown in Fig. 5(b), it is found that the vibration amplitude of the main system in the direction of the wind velocity produced by the motion of Hula-Hoops is small. However, by using one set of two units rather than one unit, the averaged amplitude of the main system in the direction of the wind still becomes small, and it is possible to have some quenching effect even if one of these devices is breaking down. Consequently, it is thought that using one set of the two units is advantageous from these viewpoints.

When the direction of the wind changes, the vortex-induced vibration in the directions of high flexural rigidity generates. It is possible to quench the vortex-induced vibration in the directions of high rigidity by using four Hula-Hoops as it is. Here, the relation about the position between the four Hula-Hoops and the main system is as it is, and the experiment about quenching of vortex-induced vibration generated in the direction of high rigidity when the direction of the wind is

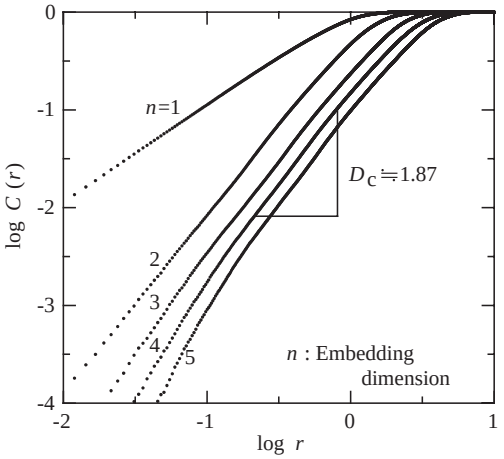

Fig. 6. Correlation dimension.

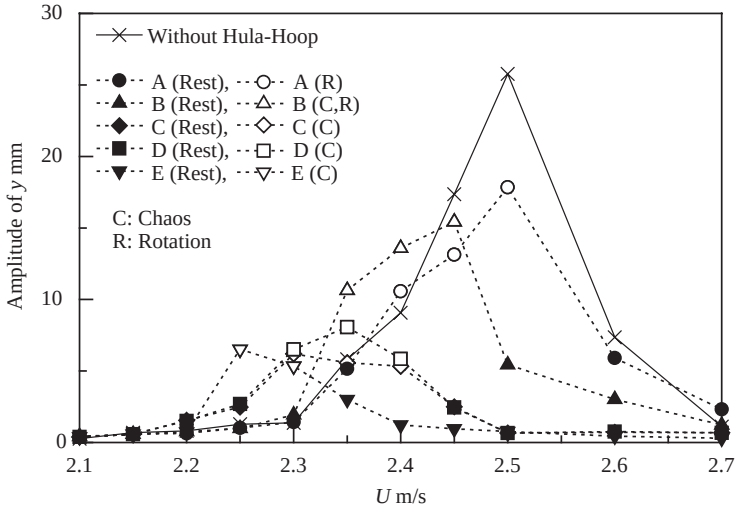

Fig. 7. Wind response curve (experiment: high rigidity direction).

changed 90° is carried out. The wind velocity response curve and the amount of power generation are shown in Figs. 7 and 8, respectively. Hula-Hoops C–E quenched the vortex-induced vibration well in Fig. 7. If Hula-Hoop C is used, the amplitude in every wind velocity has become 25% or less of the maximum amplitude in the case without a quenching device. Furthermore, as shown in Fig. 8, the amount of power generation is more than that in the case of a direction of low rigidity of Fig. 3. This is because the natural frequency of high rigidity direction is higher than that of low rigidity direction and Hula-Hoops rotate and vibrate at a higher speed. Moreover, the vibration amplitude of the direction of wind velocity was slight.

In addition, when the direction of the wind is in the middle of a direction of low rigidity and a direction of high rigidity, the measured amplitude of vortex-induced vibration is smaller than that of both vortex-induced vibrations. In such a case, the amplitude of about 7 mm or less was realized by using the set of four devices which consists of Hula-Hoops C and generators.

As mentioned above, it is made clear from the experiment that even if the direction of the wind and wind velocity changed, the quenching vibration and the power generation can be effectively performed by using four sets of devices which consist of Hula-Hoops C and generators as it is.

3. Theoretical analysis

In order to verify the result of quenching the vibration and power generation which is shown experimentally in Section 2, numerical analysis was performed using the Iwan and Blevins's model of vortex-induced vibration [5]. Because the cylinder used in the experiment is considered rigid and the steel beam fixed inside the cylinder performs a bending motion, this model can be used approximately in the analysis.

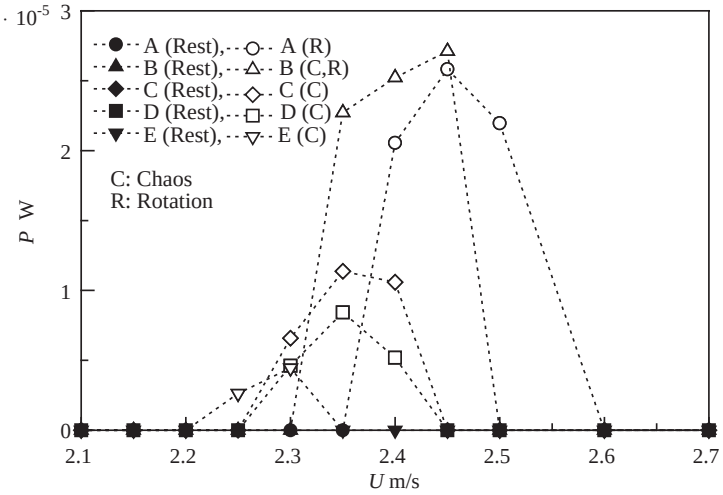

Fig. 8. Electric power (Experiment; high rigidity direction).

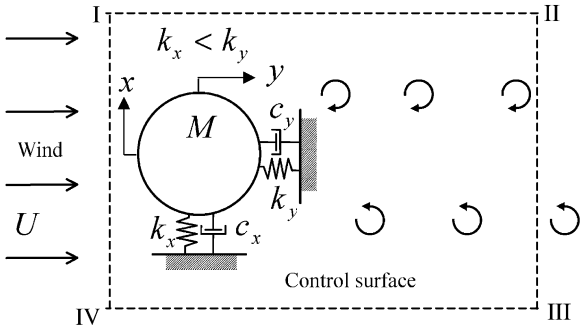

Fig. 9. Iwan and Blevins's model of vortex-induced vibration.

3.1. Iwan and Blevins's vortex-induced vibration model

The vibration of the cylinder by the Karman vortex is explained according to the Iwan and Blevins's model [4] shown in Fig. 9. According to the experiment, the direction of low flexural rigidity where the natural frequency of the main system is low is defined as the x direction, and the direction of high flexural rigidity where the natural frequency is high is defined as the y direction. At first, the vortex-induced vibration that generates in the direction of low rigidity is considered. The balance of the forces for the control volume shown in Fig. 9 becomes as follows:

$$\dot{J}_x = P_x - S_x - F_z, \tag{3}$$

where J_x is the momentum in the direction of x within the control volume, P_x is the upward pressure force acting on the fluid, and it originates in the difference of pressure which acts on sections III–IV and the pressure which acts on sections I–II. F_z is the force acting on the fluid from an object, namely this is the reaction force acting on an object from the fluid. S_x is the increasing ratio of the difference of the momentum, which flows in through sections I–IV and the

momentum, which then flows out through sections II–III; it mainly expresses the momentum change by vortex discharge. These values become as follows:

$$J_x = b_0\rho D^2\dot{z}, \quad P_x = 0, \quad F_z = b_4\rho DU(\dot{z} - \dot{x}),$$
$$S_x = K\rho U\omega_s Dz - b_1\rho UD\dot{z} + (b_2\rho D/U)\dot{z}^3,$$
$$\omega_s = 2\pi S_t U/D, \tag{4}$$

where $\dot{z}$ is a weighted average of the transverse component of the flow within the control volume, U is the wind velocity, ρ is the air density, D is a cylindrical diameter, ω_s is the angular velocity of vortex shedding, S_t is the dimensionless Strouhal number, K, b_0, b_1, b_2, b_4 are constants, and $\dot{x}$ is a velocity of the cylinder.

The following equation is obtained if Eq. (4) is substituted for Eq. (3).

$$b_0\rho D^2\ddot{z} - b_1\rho UD\dot{z} + \frac{b_2\rho D}{U}\dot{z}^3 + K\rho U\omega_s Dz = -F_z. \tag{5}$$

Moreover, when the direction of the wind changed to 90° in Fig. 9, the vortex-induced vibration of the direction of high rigidity generates and the following equation is realized:

$$F_z = b_4\rho DU(\dot{z} - \dot{y}). \tag{6}$$

Next, the elastically supported cylinder is considered. In a vortex-induced vibration of the direction of low rigidity, as the fluid force F_z of Eq. (4) acts on a cylinder with the length L, F_zL becomes the fluid force of the direction (x direction) of low rigidity. At this time, the equation of motion is expressed with the following equation:

$$M\ddot{x} + c_x\dot{x} + k_x x = F_x, \tag{7}$$

$$M\ddot{y} + c_y\dot{y} + k_y y = F_y, \tag{8}$$

where

$$F_x = b_4\rho DUL(\dot{z} - \dot{x}), \quad F_y = 0. \tag{9}$$

However, M is the mass of the cylinder, c_x, c_y, k_x, $k_y(k_x < k_y)$ are the damping coefficients and the spring constants of x, y direction of a main system, respectively. From Eqs. (7) and (8), it turns out that the cylinder is vibrated only in a perpendicular direction to the wind by F_x in the model of Iwan. On the other hand, in the case of vortex-induced vibration of the direction of high rigidity, where a wind blows from the upper part of Fig. 9, the right side of Eqs. (7) and (8) serve as the following equation:

$$F_x = 0, \quad F_y = b_4\rho DUL(\dot{z} - \dot{y}). \tag{10}$$

3.2. Equation of motion in quenching vibration

The vibrating model shown in Fig. 10 was considered. Namely, the model of the towering structure used in the experiment was approximated by the two-degree-of-freedom system that can move within a level plane. The plane consists of the direction of the wind and the perpendicular direction to the wind. Four quenching devices are installed and those consist of the same Hula-Hoops and the same generators as each other.

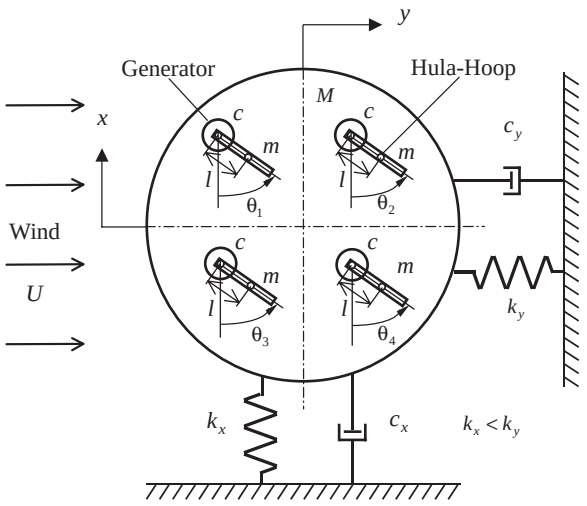

Fig. 10. Analytical model of a vibrating system.

Motion on the level surface of the system of Fig. 10 was considered. x, y and $\theta_i (i = 1, \ldots, 4)$ are the displacement of the direction of low rigidity of the main system, the displacement of the direction of high rigidity, and the angle displacement of a Hula-Hoop, respectively. $M$and m are the mass of the main system and that of the Hula-Hoop, respectively. Moreover, the stem length is l, the inertia moment of the Hula-Hoop about the axis of the center of gravity is I, the viscous damping coefficient of the Hula-Hoop resulting from power generation is c. In addition, the mass of the generator is included in the mass of the main system.

The equation of motion becomes as follows:

$$b_0\rho D^2\ddot{z} - b_1\rho UD\dot{z} + \frac{b_2\rho D}{U}\dot{z}^3 + K\rho U\omega_s Dz = -F_z, \tag{11}$$

$$(M + 4m)\ddot{x} + c_x\dot{x} + k_x x + \sum_{i=1}^{4} ml(\ddot{\theta}_i \sin\theta_i + \dot{\theta}_i^2 \cos\theta_i) = F_x, \tag{12}$$

$$(M + 4m)\ddot{y} + c_y\dot{y} + k_y y + \sum_{i=1}^{4} ml(\ddot{\theta}_i \cos\theta_i - \dot{\theta}_i^2 \sin\theta_i) = F_y, \tag{13}$$

$$(I + ml^2)\ddot{\theta}_i + c\dot{\theta}_i + ml(\ddot{x}\sin\theta_i + \ddot{y}\cos\theta_i) = 0 \quad (i = 1, \ldots, 4). \tag{14}$$

Eqs. (11)–(14) are explained briefly below. Eq. (11) means the self-excited generation of vortex, although the vortex is influenced throw F_z by the structure. On the contrary, Eqs. (12) and (13) are the equations of motion of the structure for the directions x and y, respectively, and the structure is influenced by F_x and F_y. Moreover, Eq. (14) means that the Hula-Hoop is affected by the structure parametrically. As a result, the structure is quenched by the fourth terms of the left sides of Eqs. (12) and (13) which show the influence of the Hula-Hoops.

3.3. Numerical computation method and values of parameters

The system expressed with Eqs. (11)–(14) is a non-linear seven-degree-of-freedom system. Since not only periodic solutions but also aperiodic solutions exist mostly in this system, the numerical integration of Eqs. (11)–(14) is carried out for a long time from a suitable initial condition by using the Runge–Kutta–Gill method and the converged values after a long integration is adopted as a numerical solution. The values of the used parameter correspond to those of the experiment, the mass of a main system is $M = 0.200\,\mathrm{kg}$, damping coefficient in the direction of x and y of the main system, and the spring constants of each direction are $c_x = 3.4 \times 10^{-2}\,\mathrm{N\,s/m}$, $c_y = 4.7 \times 10^{-2}\,\mathrm{N\,s/m}$, $k_x = 197.4\,\mathrm{N/m}$, $k_y = 284.2\,\mathrm{N/m}$, respectively. The diameter and the length of the cylinder are $D = 0.083$ and $L = 0.365\,\mathrm{m}$, respectively. The air density is $\rho = 1.226\,\mathrm{kg/m^3}$, and the viscous damping coefficient of the Hula-Hoop is $c = 7.5 \times 10^{-7}\,\mathrm{N\,m/s}$. Each parameter of Iwan and Blevins's vortex-induced vibration model was decided as follows. To make the maximum amplitude and its wind velocity in the case of having no quenching device agree with those of the experimental results, $S_t = 0.2030$, $K = 0.38$, $b_0 = 0.30$, $b_1 = 0.35$, $b_2 = 0.11$, $b_4 = 0.13$ are used for the vortex-induced vibration in the direction of low rigidity, on the other hand, $S_t = 0.2035$, $K = 0.68$, $b_0 = 0.53$, $b_1 = 0.49$, $b_2 = 0.10$, $b_4 = 0.10$ are used for the vortex-induced vibration in the direction of high rigidity.

4. Results of numerical analysis

First, the quenching of the vortex-induced vibration in the direction of low rigidity was considered. In the case of having no quenching device, the vibration amplitude in the direction of high rigidity obtained numerically was zero. On the other hand, the vibration amplitude in the direction of high rigidity was measured slightly in the experiment. This difference originates on Iwan and Blevins's vortex-induced vibration model that considers only the vibration of the main system transverse to the wind direction. When the quenching and power generation devices are installed, the obtained solutions by the numerical computation are classified into periodic solutions and aperiodic ones. The typical waveforms of the vortex-induced vibration in the direction of low rigidity are shown in Fig. 11. These are the waveforms that have almost the maximum amplitude of displacement and have a round number of wind velocity in the wind response curves as shown in Fig. 13 later. From the upper row in order, they are a displacement waveform of x direction of the main system and that of y direction, and angular velocity waveforms of four Hula-Hoops. In Fig. 11(a), the main system is a periodic vibration of 4.9 Hz and Hula-Hoops rotate to one direction, although those angular velocities deviate. In Fig. 11(b), each Hula-Hoop repeats standstill, vibration, and rotation aperiodicaly, while the main system vibrates like a beat according to the motion of Hula-Hoops. The Poincaré map corresponding to this motion is shown in Fig. 12. The abscissa and the ordinate of the figure are the displacements of the main system at the maximum points in its time history, namely n times and $n+1$ times one, respectively ($n = 1, 2, \ldots, 2000$). A narrow channel can be seen between the straight line of the unit inclination and the Poincaré map. It turns out that this motion is the intermittent chaos. The numerically calculated maximum Lyapunov exponent of this solution is 0.0201. This intermittent chaos is generated by the interaction between the main system and the Hula-Hoops. The

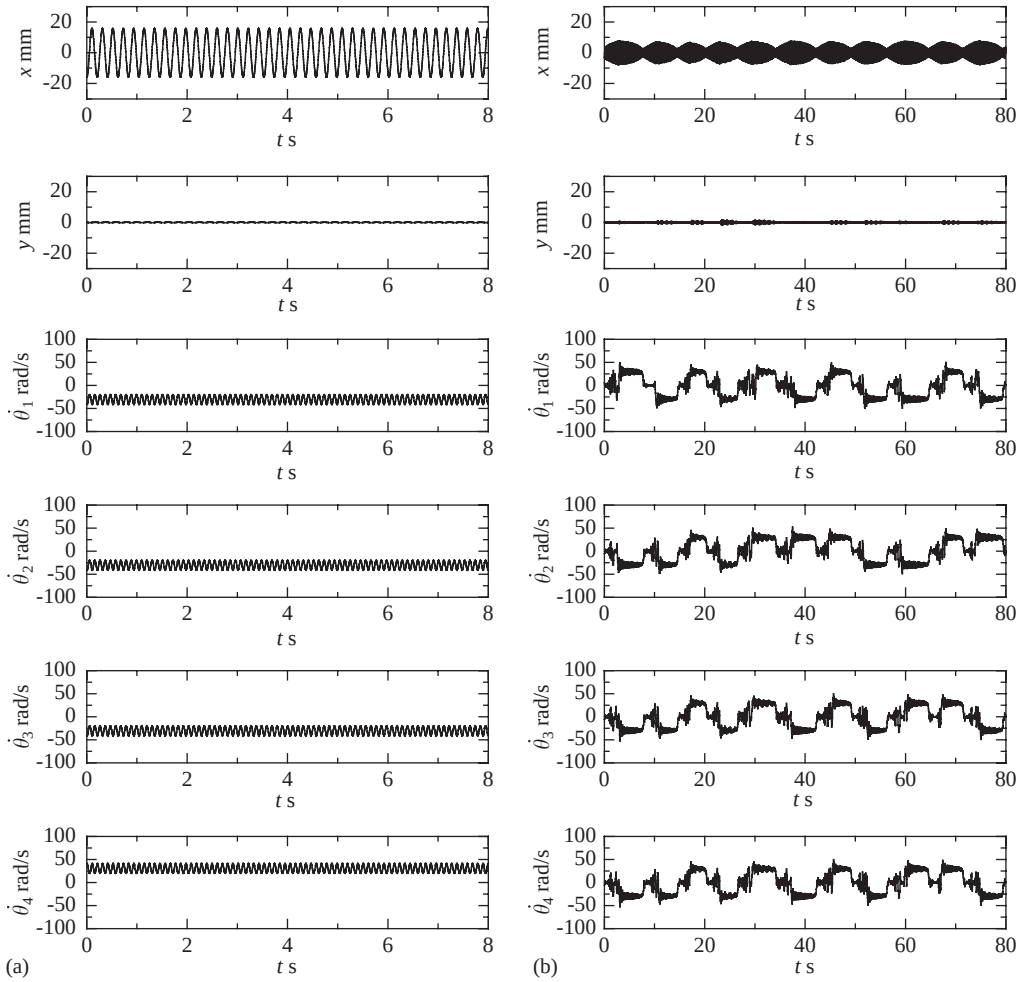

Fig. 11. Calculated waveforms with Hula-Hoops: (a) periodic solution (Hula-Hoop B, $U = 2.00\,\mathrm{m/s}$); (b) chaos (Hula-Hoop C, $U = 2.00\,\mathrm{m/s}$).

Hula-Hoops absorb the vibration energy from the main system by rotating. After the amplitude of the main system decreases, the Hula-Hoops are not able to maintain the rotation and become still. Then the amplitude of main system increases slowly and the Hula-Hoops start to vibrate and shift to a rotation. In this way, the Hula-Hoops repeat standstill, vibration, and rotation. This is the mechanism of intermittent chaos. In the numerical analysis, when the same suitable initial conditions were given for the four Hula-Hoops, the motion of each Hula-Hoop was completely in agreement even in the case of chaos. On the other hand, if the initial conditions of the four Hula-Hoops are different each from the other, the motion of each Hula-Hoop was not in agreement. In a rotational solution, as shown in Fig. 11(a), the four Hula-Hoops may rotate in an opposite direction mutually. In the solution of chaos, if the averaged value in a sufficient period of time is taken, the difference between the quenched amplitude in the cases where it calculates from the same initial conditions and that from the different initial conditions was several percent, and

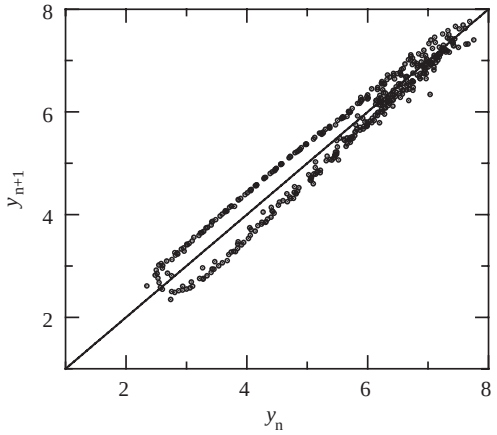

Fig. 12. Poincaré map.

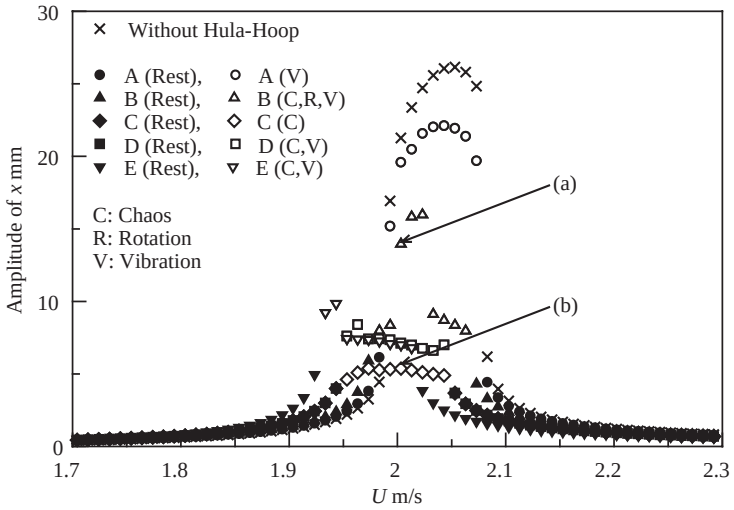

Fig. 13. Wind response curve (low rigidity direction).

the difference in the power generation was also several percent. Consequently, the different initial conditions are adopted for the four Hula-Hoops in the numerical analysis, and the results obtained after a sufficient period of time numerical integration are shown.

The wind velocity response curve of the vortex-induced vibration generated in the direction of low rigidity is shown in Fig. 13 and the amount of power generated is shown in Fig. 14. The definitions of the marks in the figures are the same as those of Figs. 2 and 3. However, since the solutions that the Hula-Hoops did not rotate but vibrate existed slightly, these solutions are shown by "V". The displacement amplitude in the case of chaos is calculated by (average value of local maximum−average value of local minimum)/2 as in the experiment. The amount of power generation per unit time (W) shown in Fig. 14 is calculated as follows. If the load for power

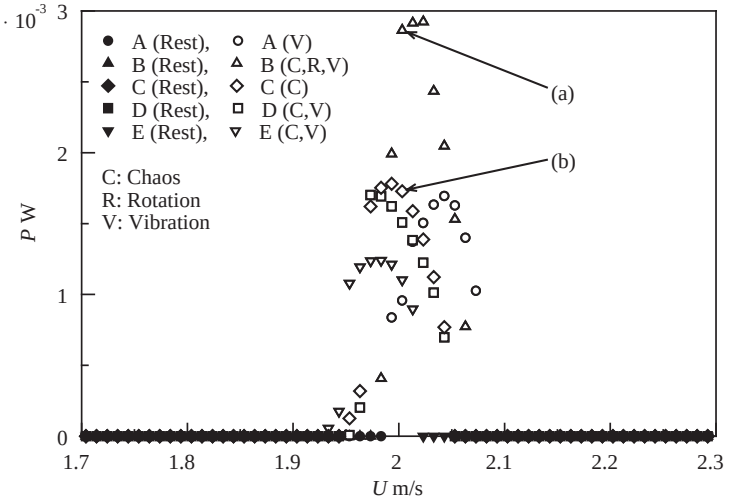

Fig. 14. Electric power (low rigidity direction).

generation is considered to be a viscous damping force, the sum of the power generation P' (J) generated in the generators for a certain number of seconds T (s) is defined by the next equation using the coefficient c (kg m^2/s) and the rotating angular velocity $\dot{\theta}_i$ of a Hula-Hoop ($i = 1, \ldots, 4$):

$$P' = \sum_{i=1}^{4} \int_{\theta_i(0)}^{\theta_i(T)} c\dot{\theta}_i \, \mathrm{d}\theta_i = \sum_{i=1}^{4} c \int_0^T \dot{\theta}_i^2 \, \mathrm{d}t. \tag{15}$$

Therefore, the amount of power generation per unit time P (W) is expressed as follows:

$$P = \frac{P'}{T} = \sum_{i=1}^{4} \frac{c}{T} \int_0^T \dot{\theta}_i^2 \, \mathrm{d}t. \tag{16}$$

The time T of the upper equation is a period of periodic solution, or if the solution is chaos, it is a sufficient period of time like that used in calculating the average amplitude.

The Hula-Hoop C has the greatest quenching effect in Fig. 13 and this Hula-Hoop is considered the optimum one. It turns out that the quenched amplitudes are 25% or less of the maximum amplitude in the case without the quenching device (about 26 mm in $U = 2.05$ m/s) over all of the wind velocity ranges in Fig. 13. The results about quenching vibration obtained by numerical computation are qualitatively in agreement with the experimental result. However, the motion of a Hula-Hoop does not correspond in part, namely, the vibrating solution is obtained in calculation.

In addition, many cases were calculated, as examples, several pieces of the Hula-Hoops were replaced with those which were not optimum, or combinations of longer stem length and shorter one than the optimum one were tried. However, those results were not better than the optimum case where the same four optimum Hula-Hoops were used. The motion in the optimum quenching is chaos not only in the experiment but also in the numerical computation. On the other hand, when the Hula-Hoops are not optimum, there is a possibility that the motion becomes vibration

or rotation. This result is the same as that of the previous paper that dealt with the quenching problem of a one-degree-of-freedom self-excited system [14].

Next, it is seen that Hula-Hoop B generates the greatest amount of power in Fig. 14. Although the vibrating state at the time of optimum quenching is chaos, the regular rotation of the Hula-Hoop is better for power generation. Therefore, the condition of optimum quenching is different from the condition of the maximum amount of power generation. The amount of power generation in the experiment is smaller than that in the numerical computation of Fig. 14. This is because the efficiency of the motor used as a generator is very low in the low rotational speed.

Referring to Fig. 11, the quenching effect of the Hula-Hoops shown in Fig. 13 and the amount of power generation shown in Fig. 14 are explained as follows. At first, the vibration energy of the main system is absorbed by the kinetic energy of the Hula-Hoops and the damping energy for power generation of the generators. For example, since the masses of the Hula-Hoops are small in Fig. 11(a), the kinetic energies of the Hula-Hoops are small and the vibration energy of the main system is not absorbed fully, but the regular rotation of the Hula-Hoops is possible and the amount of power generation is large as shown in Fig. 14(a). On the other hand, since the masses of the Hula-Hoop are large in the example of Fig. 11(b), the vibration energy of the main system can be absorbed enough as the kinetic energies of the Hula-Hoops as shown Fig. 13(b). If the amplitude of a main system becomes small by the rotation of the Hula-Hoops, the Hula-Hoops are stopped also. If the Hula-Hoops stand still, the quenching effect is lost and the amplitude of the main system increases slowly. Since the amplitude of the main system becomes large to some extent for a while, the Hula-Hoops begin vibrating and shift to a rotation. Hula-Hoops repeat these motions of rotation, stillness, and vibration aperiodically, and the mean amplitude of the main system becomes small as a result. However, since power generation is impossible in a state when the Hula-Hoops are standing still, the average value of the amount of power generation per unit time is small as shown Fig. 14(b). Concerning the vibration of the main system in the direction of the wind velocity, the amplitude is very small and is smaller than that in the experiment as shown in Fig. 11(a) and (b).

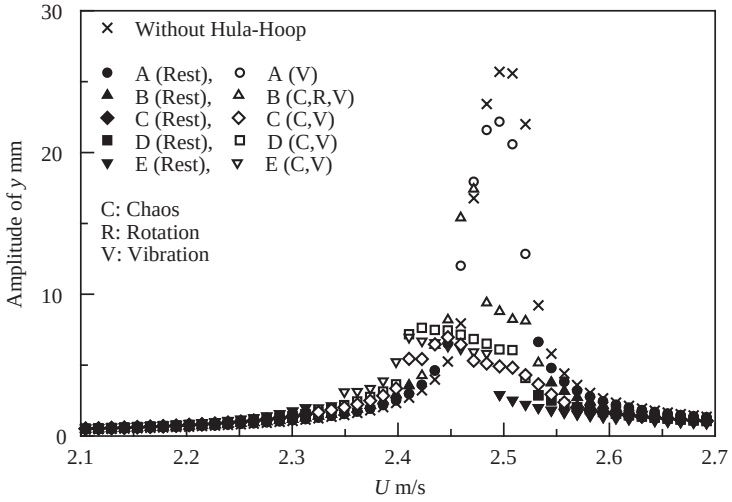

Fig. 15. Wind response curve (high rigidity direction).

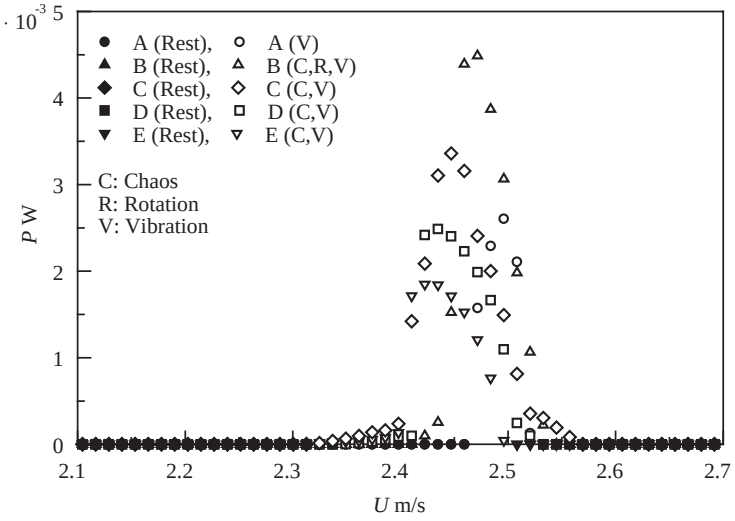

Fig. 16. Electric power (high rigidity direction).

Moreover, the numerical computation of the vortex-induced vibration in the direction of high rigidity is performed, where the direction of the wind velocity is changed 90° from the direction where the vortex-induced vibration of low rigidity is generated. The wind response curve is shown in Fig. 15. This figure shows that the optimum Hula-Hoop is type C as in the case of the vortex-induced vibration in the low rigidity direction. The amount of power generation is shown in Fig. 16. Those amounts are larger than those in the case of a direction of low rigidity. These numerical computation results are well in agreement with the experimental results qualitatively.

As mentioned above, it became clear that it is possible to quench the vibration of a towering structure effectively and to generate electric power simultaneously by using four pieces of quenching and power generating devices from the experiment and numerical computations.

5. Conclusion

The research about quenching the vortex-induced vibration of a towering structure and power generation by using four pieces of quenching and power generating devices made of Hula-Hoops and generators were performed, the results of this research are summarized as follows:

(1) It is confirmed that these devises were able to quench the vibration of a structure over a wide range of wind velocities where the vortex-induced vibration was a problem and were also effective for the case when the direction of the wind velocity changed.
(2) This quenching problem is a quenching utilizing chaos while the optimum quenching conditions are not necessarily in agreement with those of a maximum power generation condition.
(3) The amplitude of the vibration of the main system in the direction of the wind velocity, which is generated by the centrifugal force of the Hula-Hoops was small and did not become a problem compared with the amplitude in the transverse direction of the wind velocity.

References

[1] G. Birkhoff, Formation of vortex streets, *Journal of Applied Physics* 24 (1953) 98–103.
[2] M. Funakawa, The vibration of a cylinder caused by wake in a flow, *Bulletin of the JSME* 12–53 (1969) 1003–1010.
[3] R.T. Hartlen, I.G. Currie, Lift oscillation model for vortex-induced vibration, *Journal of the Engineering Mechanics Division ASCE* 96 (1970) 577–591.
[4] R.A. Skop, O.M. Griffin, On a theory for the vortex-excited oscillations of flexible cylindrical structures, *Journal of Sound and Vibration* 41 (3) (1975) 263–274.
[5] W.D. Iwan, R.D. Blevins, A model for vortex induced oscillation of structures, *Journal of Applied Mechanics* 41 (3) (1974) 581–585.
[6] E.H. Dowell, Non-linear oscillator models in bluff body aeroelasticity, *Journal of Sound and Vibration* 75 (2) (1981) 251–264.
[7] Z.G. Hanko, Vortex induced vibration at low-head wiers, *Proceedings of the American Society of Civil Engineers Hydraulics Division* 93 (1967) 255–270.
[8] D.E. Walshe, L.R. Woolton, Preventing wind induced oscillations of structures of circular section, *Proceedings of the Institution of Civil Engineers* (*London*) 47 (1970) 1–24.
[9] L. Andersen, N.W. Wirch, A.H. Hansen, J.-O. Skibelund, Response analysis of tuned mass dampers to structures exposed to vortex loading of Simiu-Scanlan type, *Journal of Sound and Vibration* 239 (2) (2001) 217–231.
[10] M. Nishioka, M. Asai, S. Yoshida, Control of flow separation by acoustic excitation, *American Institute of Aeronautics and Astronautics Journal* 28 (1990) 1909–1915.
[11] A. Baz, J. Ro, Active control of flow-induced vibrations of a flexible cylinder using direct velocity feedback, *Journal of Sound and Vibration* 146 (1) (1991) 33–45.
[12] K. Venkatraman, S. Narayanan, Active control of flow-induced vibration, *Journal of Sound and Vibration* 162 (1) (1993) 43–55.
[13] V. Gattulli, R. Ghanem, Adaptive control of flow-induced oscillations including vortex effects, *International Journal of Non-Linear Mechanics* 34 (1999) 853–868.
[14] Y. Yoshitake, A. Sueoka, T. Moriyama, M. Yamasaki, Quenching of self-excited vibrations and generation of electricity by using Hula-Hoop, *Transactions of JSME* 66–646 (2000) 1785–1792 (in Japanese).
[15] A. Kusko, *Solid-State DC Motor Drives*, The MIT Press, Cambridge, MA, 1969.